RESEARCH PAPER | Psychology | Volume : 3 | Issue : 10 | Oct 2013 | ISSN - 2249-555X

# Structural and Electrical Properties of Thermally Evaporated SnxSe1-x Thin Films

KEYWORDS

| Bushra A. Hasan | Ghuson H. Mohamed | Amer A.Ramadhan |
|---|---|---|
| University of Baghdad, College of Science, Department of Physics | University of Baghdad, College of Science, Department of Physics | University of Baghdad, College of Science, Department of Physics |

**ABSTRACT** *Tin Selenide SnxSe1-x thin films were prepared from the alloy compound material by thermal evaporation method, to study the effect of tin content (x=0.1 ,0.5, and 0.7)and on its structural, and electrical properties. Thin films SnxSe1-x thicknesses of 300 nm, were grown on glass substrate held at room temperature. X-ray diffraction, D.C conductivity , and Hall effect measurements, were used to characterize the thin films. The XRD studies reveal that Sn0.5Se0.5 and Sn0.7Se0.3 films are crystalline with orthorhombic structure. while Sn0.1Se0.9 films were crystalline with hexagonal structure. Microstructure parameters such as crystallite size, and dislocation density were calculated and found to depend upon deposition parameters. The plot of conductivity with reciprocal temperature suggests, there are two activation energies Ea1 and Ea2 for SnxSe1-x for all x content values transport to one activation energy Ea1 at high tin content which decreases with increasing tin content .Hall Effect measurements showed that the SnxSe1-x thin films were n -type semiconductors at x=0.1 convert to p-type semiconductors at x=0.5 and 0.7.*

**Introduction**

Tin monoselenide (SnSe) and tin diselenide ($SnSe_2$) have attracted wide-spread attention due to their electronic and optical properties [1]. The narrow band gap energy (between 1-2 eV) makes them capable of absorbing a major part of solar energy and thus potential candidates for photovoltaic applications [2]. Tin diselenide is an n-type semiconductor and its band gap is ~0.9 eV. $SnSe_2$ presents a hexagonal $CdI_2$-type crystal structure characterized by strongly bonded two-dimensional Sn-Se-Sn sandwiches, which are weakly coupled by Van der Waals forces. In the present work, we have studied the phase change properties of SnSe-$SnSe_2$ upon different tin content by thermal evaporation of $Sn_xSe_{1-x}$ alloys. The structural, and electrical properties of the films were analyzed and discussed.

**Experimental procedure**

Prior to deposition, the substrates were cleaned in with cleaner solution, distilled water and followed by alcohol using ultrasonic bath.

The alloys of $Sn_xSe_{1-x}$ were prepared by quenching technique. The exact amount of high purity (99.999%) (Sn and Se) elements accordance with their atomic percentages (Sn: Se = 0.1:0.9, 0.5:0.5 and 0.7:0.3) were weighed using an electronic balance with the least count of ($10^{-4}$ gm). The mixed elements were sealed in evacuated (~$10^{-3}$ Torr) quartz ampoule (length ~ 25 cm and internal diameter ~ 8 mm). The ampoules which containing the elements were heated to 650C for x=0.1 and x=0.7 and 800 for x=0.5 for 5 hours then cooled to room temperature. The temperature of the furnace was raised at a rate of10°C/min. During heating the ampoules are constantly rocked .This is done to obtain homogeneous glassy alloys.

The vacuum unit system, which is used to prepare thermally evaporated $Sn_xSe_{1-x}$ films, was supplied by Edward coating unit (model 606) under high vacuum ($10^{-5}$m bar) which was provided by rotary and diffusion pump.

Crystal structure were investigated by means of a X-ray diffraction XRD Shimadzu 6000 Japan using $CuK_{\alpha 1}$, λ=1.5405Å). To study the electrical properties for the films Ohmic contacts for the prepared films are produced by evaporating (Al) electrodes of 300 nm thickness, by means of thermal evaporation methods, using Edward coating unit (model 606), then the d.c conductivity (σ) have been studied using the electrical circuit which is consists of oven type Herease and keithley (616). The thickness of the prepared films has been determined using Fizeau fringes of equal thickness are obtained in an optical aperture. The film thickness (t) is given by:

$$t = \frac{\lambda}{2} \cdot \frac{\Delta X}{X}$$

Where ΔX is the shift between the interference fringes, X is the distance between the interference fringes and λ is the He: Ne wavelength (5893 Å).

**Results and Discussion**

Fig. 1 shows the X-ray diffraction pattern recorded on syntheses $Sn_xSe_{1-x}$ powder with different tin content. The identification of the crystalline phases in the ingot leads to the conclusion that the major phase consists of the $Sn_{0.1}Se_{0.9}$ is hexagonal structure (Fiche No.23-0602). A minor phase of $Sn_{0.1}Se_{0.9}$ with orthorhombic structure(Fiche No. 38-1055) was revealed. The increase of tin content in the ingot led to domination orthorhombic structure on the expense of hexagonal phase. X-ray diffraction (XRD) patterns of $Sn_xSe_{1-x}$ thin films with different tin content (0.1 , 0.5 , and 0.7) in thickness of 300 nm, deposited at room temperature are shown in Figure 2 .It is clear that the tin content has significant influence on the quality of the films. For instance, the films grown with low tin content (x=0.1) have low crystallinity in compared with film rich in tin content (0.5 and 0.7). XRD of the (Fig. 2) confirms the elemental ratio of Sn:Se. $Sn_{0.1}Se_{0.9}$ has a hexagonal unit cell and is a layered crystal with repeating Se-Sn-Se tri layers. The intense (101) and (0 0 3) peaks in the XRD pattern indicate that our thin films preferentially oriented in the (101) plane.

The prepared $Sn_{0.5}Se_{0.5}$ and $Sn_{0.7}Se_{0.3}$ have orthorhombic structure and polycrystalline in nature with diffraction peaks correspond to (011), (111), and (411) reflections at around 2 θ of $29.5^0$,$30.5^0$ and $43.4^0$ respectively which is good agreement with slandered with the standard JCPDS data [card no. 32-1382]. The preferred orientation along (111) plane increases with increase of tin content in the prepared films , which indicates that the addition of tin led to increases the degree of crystallinity . A similar result with preferred orientation of (111) plane was also reported by Singh and Bedi[3] and Z. Zainal et al.[4] for the SnSe

Volume : 3 | Issue : 10 | Oct 2013 | ISSN - 2249-555X

thin films grown by the vacuum evaporation technique. A similar preferred orientation of grains along the (111) plane in SnSe film was observed in the evaporated SnSe thin films by Bhatt et al. [5] and by Dang Tran Quan [6]. On the other hand, H. Chandra et al. [7] had observed (400) diffraction plane for films grown by flash evaporation technique and Teghil et al. [8] had reported orientation of grains along (011) and (200) crystallographic planes in the SnSe thin film prepared by laser ablation method. The various preferred orientation of grains reported for SnSe films deposited using different techniques indicate that the mode of deposition plays decisive role on the growth structure of the films.

The inter-planar spacing ($d_{hkl}$) calculated for the all the planes having different tin content using the Bragg's relation are presented in Table(2). The crystalline size was estimated from the full width at half maximum (FWHM) of the peak using Scherrer's formula[9]:

$$D = \frac{0.94\lambda}{\beta\cos\theta}$$

where, $\lambda$ is the wavelength of the X-ray, $\theta$ is Bragg's angle, and $\beta$ is the FWHM of peak. The dislocation density ($\delta$) defined as the length of dislocation lines per unit volume of the crystal is given by the Williamson and Smallman's relation[10],

$$\delta = \frac{n}{D^2}$$

where, n equals to unity, giving a minimum dislocation density and D is the crystalline size. The values of crystalline size (D) and dislocation density ($\delta$) are also given in the Table (2).

It is observed that the crystalline size increases from14 to 31 nm with the increase of tin content from 0.5 to 0.7. In polycrystalline samples, dislocated atoms occupy the regions near the grain boundary. Generally the dislocation density is inversely proportional to crystalline size so it as observed that dislocation density decreases with increase of tin content.

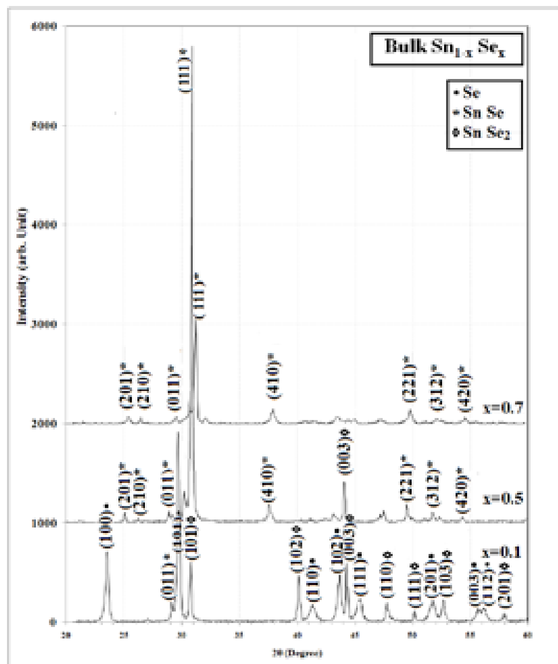


**Fig (1) XRD for bulk $Sn_xSe_{1-x}$ with different x content.**

**Table 1. Structural Parameters viz. Inter-planar Spacing, Crystalline Size, and Dislocation Density of bulk $Sn_xSe_{1-x}$ with different tin content (x=0.1, 0.5 and 0.7) .**

| x | 2θ (Deg.) | FWHM (Deg.) | $d_{hkl}$ Exp (Å) | D(nm) | $d_{hkl}$ Std (Å) | hkl | phase |
|---|---|---|---|---|---|---|---|
| 0.1 | 23.58 | 0.39 | 3.771 | 19.5 | 3.780 | (100) | SnSe |
| | 29.16 | 0.22 | 3.060 | 34.6 | 3.054 | (011) | SnSe |
| | 29.72 | 0.28 | 3.004 | 27.7 | 3.005 | (111) | SnSe |
| | 30.84 | 0.28 | 2.897 | 27.8 | 2.910 | (101) | $SnSe_2$ |
| | 40.17 | 0.28 | 2.243 | 28.5 | 2.250 | (102) | $SnSe_2$ |
| | 41.40 | 0.61 | 2.179 | 13.0 | 2.184 | (110) | SnSe |
| | 43.74 | 0.45 | 2.068 | 18.0 | 2.072 | (411) | SnSe |
| | 44.30 | 0.22 | 2.043 | 36.2 | 2.050 | (003) | $SnSe_2$ |
| | 45.47 | 0.39 | 1.993 | 20.7 | 1.998 | (111) | SnSe |
| | 47.77 | 0.39 | 1.903 | 20.9 | 1.910 | (110) | $SnSe_2$ |
| | 50.17 | 0.22 | 1.817 | 37.0 | 1.820 | (111) | $SnSe_2$ |
| | 51.79 | 0.61 | 1.764 | 13.5 | 1.766 | (201) | SnSe |
| | 52.68 | 0.28 | 1.736 | 29.9 | 1.740 | (103) | $SnSe_2$ |
| | 55.64 | 0.50 | 1.650 | 16.8 | 1.650 | (003) | SnSe |
| | 56.15 | 0.56 | 1.637 | 15.2 | 1.637 | (112) | SnSe |
| | 57.93 | 0.34 | 1.591 | 25.5 | 1.590 | (201) | $SnSe_2$ |
| 0.5 | 25.14 | 0.22 | 3.540 | 34.3 | 3.515 | (201) | SnSe |
| | 26.26 | 0.22 | 3.391 | 34.4 | 3.376 | (210) | SnSe |
| | 28.94 | 0.22 | 3.083 | 34.6 | 3.054 | (011) | SnSe |
| | 30.28 | 0.22 | 2.949 | 34.7 | 2.949 | (111) | SnSe |
| | 30.89 | 0.22 | 2.892 | 34.7 | 2.854 | (101) | $SnSe_2$ |
| | 37.60 | 0.34 | 2.390 | 23.6 | 2.360 | (410) | SnSe |
| | 44.08 | 0.22 | 2.053 | 36.1 | 2.050 | (003) | $SnSe_2$ |
| | 49.50 | 0.22 | 1.840 | 36.9 | 1.799 | (221) | SnSe |
| | 51.73 | 0.28 | 1.766 | 29.8 | 1.749 | (312) | SnSe |
| | 54.30 | 0.34 | 1.688 | 25.1 | 1.689 | (420) | SnSe |
| 0.7 | 25.42 | 0.28 | 3.501 | 27.5 | 3.515 | (201) | SnSe |
| | 26.54 | 0.17 | 3.356 | 45.9 | 3.376 | (210) | SnSe |
| | 29.50 | 0.34 | 3.026 | 23.1 | 3.054 | (011) | SnSe |
| | 30.56 | 0.28 | 2.923 | 27.8 | 2.949 | (111) | SnSe |
| | 31.17 | 0.28 | 2.867 | 27.8 | 2.854 | (101) | $SnSe_2$ |
| | 37.93 | 0.45 | 2.370 | 17.7 | 2.360 | (410) | SnSe |
| | 49.78 | 0.34 | 1.830 | 24.6 | 1.799 | (221) | SnSe |
| | 52.07 | 0.34 | 1.755 | 24.8 | 1.749 | (312) | SnSe |
| | 54.58 | 0.34 | 1.680 | 25.1 | 1.689 | (420) | SnSe |

Volume : 3 | Issue : 10 | Oct 2013 | ISSN - 2249-555X

**Fig. (2) X-ray diffraction pattern for $Sn_xSe_{1-x}$ films thickness of 300nm with different x content.**

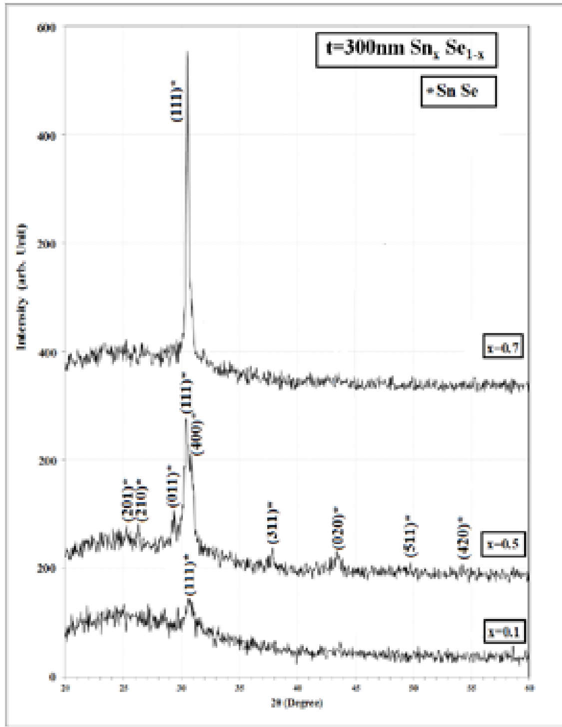


Table 2. Structural Parameters viz. Inter-planar Spacing, Crystalline Size, and Dislocation Density of $Sn_xSe_{1-x}$ films thickness of 300nm with different tin content (x=0.1, 0.5 and 0.7) deposited at room temperature.

| x | 2θ (Deg.) | FWHM (Deg.) | $d_{hkl}$ Exp (A) | D(nm) | $d_{hkl}$ Std (A) | hkl | Phase | δx10$^{-2}$(nm)$^{-2}$ |
|---|---|---|---|---|---|---|---|---|
| 0.1 | 30.67 | 0.67 | 2.913 | 11.6 | 2.949 | (101) | $SnSe_2$ | 4.31 |
| 0.5 | 25.31 | 0.39 | 3.516 | 19.6 | 3.515 | (201) | SnSe | 2.55 |
| | 26.31 | 0.28 | 3.384 | 27.5 | 3.376 | (210) | SnSe | 1.81 |
| | 29.39 | 0.34 | 3.037 | 23.1 | 3.054 | (011) | SnSe | 2.16 |
| | 30.39 | 0.55 | 2.939 | 14.1 | 2.949 | (111) | SnSe | 3.45 |
| | 30.89 | 0.28 | 2.892 | 27.8 | 2.854 | (400) | SnSe | 1.79 |
| | 37.88 | 0.45 | 2.373 | 17.7 | 2.382 | (311) | SnSe | 2.82 |
| | 43.41 | 0.50 | 2.083 | 16.0 | 2.095 | (020) | SnSe | 3.12 |
| | 49.72 | 0.22 | 1.832 | 36.9 | 1.829 | (511) | SnSe | 1.35 |
| | 54.25 | 0.39 | 1.690 | 21.5 | 1.689 | (420) | SnSe | 2.32 |
| 0.7 | 30.54 | 0.25 | 2.924 | 31.0 | 2.949 | (111) | SnSe | 1.61 |

Fig. 3 shows the temperature dependence of D.C conductivity ($\sigma_{D.C}$) of $Sn_xSe_{1-x}$ films with different x content (0.1, 0.5 , and 0.7) deposited at room temperature. The plot of ln $\sigma_{D.C}$ vs. 1000/T is straight line indicating that conduction is an activated process having activation energy in the temperature range 300- 520K. Therefore, ($\sigma_{D.C}$) can be expressed by the usual relation :

$$\sigma = \sigma_0 \exp(-\frac{E_a}{kT})$$

Where $E_a$ is the activation energy for dc conduction and k is the Boatman's constant. The value of $E_a$ is obtained from the slope of the plot of Fig. 3. It is well known that conductivity depends on the temperature, carrier concentration and mobility. In a semiconductor, carrier concentration is a rapidly increasing function of temperature in the 'intrinsic' region. This increase is due to thermal excitation of electrons, either from imperfections or across the band gap. It is clear from Fig.3 that the conductivity increases as the temperature increases, showing semiconducting behavior of the $Sn_xSe_{1-x}$ thin films. It is clear that this figure is characterized by two stages of conductivity for low tin content (0.1 and 0.5)converts to one stage for high tin content(0.7).This results come from the structural enhancement through out increase of grain size. Table (3) declares the values of D.C electrical conductivity ($\sigma_{D.C}$) ,the activation energies ( $E_a$) for all samples . The observed activation energies were attributed to the shallow acceptor states due to the Selenium vacancies. The increase in conductivity with increasing temperatures can be attributed to the improvement of the crystallization.

On the other hand the values of ( $E_a$) declares to decrease with increase of tin content , this come from lowering of potential barrier accompanies tin addition .The electrical conductivity of $Sn_xSe_{1-x}$ films was measured by F. Sava et al [11] is high ($\sigma$ = 0.1 $\Omega^{-1}cm^{-1}$) and this value places $Sn_xSe_{1-x}$ in the group of semiconducting - semi-metallic materials, while the activation energy for conduction for a PLD film was situated between 0.055 eV for temperatures around the room temperature and 1.587 eV for temperatures around 200 °C.

Our data for Hall effect measurements referrers that $Sn_xSe_{1-x}$ film with low tin content (x=0.1) was n-type ($R_H$ is negative ) i.e. there is inverse relation between the current (I) and Hall voltage ($V_H$),thus the created electric field obstructs the passage of the charge carriers (electrons) consequently the out put current will be reduced with increasing the applied electrical field .While $Sn_xSe_{1-x}$ film converts to p-type ($R_H$ is positive ) with the increase of tin content (x=0.5,0.7), here there is direct relation between the current and Hall voltage. Our explanation is the transformation from hexagonal phase related with high Se content to orthorhombic phase related with high tin content is responsible about converting from p-type conductance to n-type conductance of the $Sn_xSe_{1-x}$ film. The density of charge carriers ($n_H$)and the mobility of Hall($\mu_H$ ) were measured .Table (4) declared that ($n_H$) increases while Hall mobility of charge carriers ($\mu_H$) decreases with the increase of tin content (see Table (4)),this is attributed to lowering of potential barriers which results from the increase of grain size and increasing of electrical conductivity.

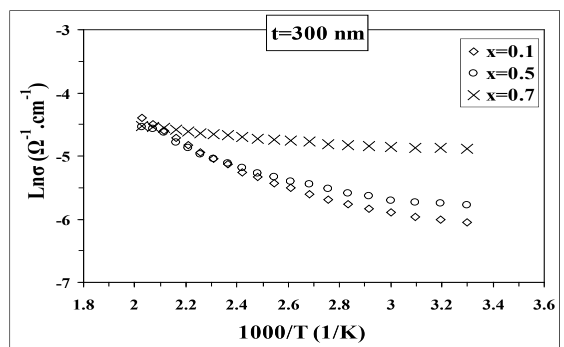


**Fig. (3) Ln (σ) Versus reciprocal of Temperature for 100nm $Sn_xSe_{1-x}$ thin films with different x content.**

**Table (3) the values of $E_{a1}$ and $E_{a2}$ and these ranges for $Sn_xSe_{1-x}$ films with different x content.**

| x | $Ea_1$ (eV) | Temp. Range (K) | $Ea_2$ (eV) | Temp. Range (K) |
|---|---|---|---|---|
| 0.10 | 0.049 | 303-363 | 0.144 | 363-483 |
| 0.50 | 0.032 | 303-363 | 0.113 | 363-483 |
| 0.70 | 0.092 | 303-483 | - | - |

Volume : 3 | Issue : 10 | Oct 2013 | ISSN - 2249-555X

**Table (4) Hall Effect measurements for $Sn_xSe_{1-x}$ thin films with different x content.**

| x | $\sigma_{RT}$(ohm. cm)$^{-1}$ | $R_H$(cm$^3$/C) | n (cm$^{-3}$)*10$^{12}$ | type | $\mu_H$ (cm$^2$/V. sec) |
|---|---|---|---|---|---|
| 0.10 | 0.0024 | -1.58E+05 | 39.6 | n | 373 |
| 0.50 | 0.0031 | 1.08E+05 | 57.9 | p | 336 |
| 0.70 | 0.0075 | 2.03E+04 | 307.9 | p | 153 |

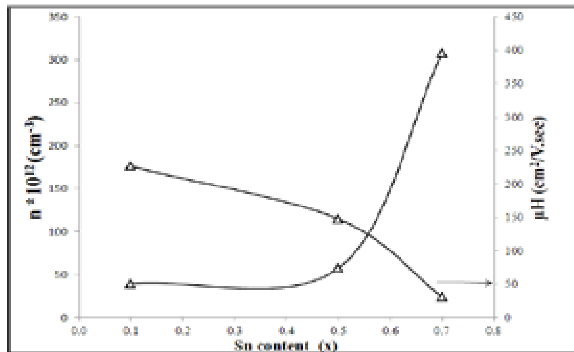


**Fig. (4) the variation of carrier concentration and mobility versus the Sn content for $Sn_xSe_{1-x}$ thin films.**

**Conclusions:**
The increase of tin content in $Sn_xSe_{1-x}$ films modified the structure through phase transformation from hexagonal to orthorhombic. Activation energy calculated from temperature dependent conductivity measurements was found to be in the range 0.14-0.09 eV .

**REFERENCE** 1. Y. Bertrand, G. Leveque, C. Raisin and F. Levy,J.Phys.C.Solid State Phys.12, 2907 (1979). | 2. M.R. Aguiar, R. Caram, M.F. Oliveira and C.S.Kiminami, J.Mater.Sci. 34, 4607 (1999). | 3. J. P. Singh and R. K. Bedi, Tin selenide films grown by hot wall epitaxy, J. Appl. Phys., 68, 2776-2779. 1990. | 4-Z. Zainal, N. Saravanan, K. Anuar, M. Z. Hussein and W. M. M. Yunus, 2003, Tin Selenide thin films prepared through combination of chemical precipitation and vacuum evapora-tion technique, Mater.Sci., , 2003, 21(2), 225-233. | 5. V. P. Bhatt, K. Gireesan, and C. F. Desai, Cryst. Res. Technol. 24, 187 (1989). | 6. D. T. Quan, Phys. Status Solidi A 86, 421 (1984). | 7. G. H. Chandra, J. Naveen Kumar, N. Madusudhana Rao, and S. Uthanna, J. Cryst. Growth 306, 68 (2007). | 8. R. Teghil, A. Santagata, V. Marotta, S. Orlando, G. Pizzella, A. Giardini-Guidoni, and A. Mele, Appl. Surf. Sci. 90, 505 (1995). | 9. B. D. Cullity, Elements of X-ray diffraction, Addi-son-Wesley Publishing Co., Inc., Reading, Massachusetts,1956. | 10. G. K. Williamson and R. E. Smallman, III. Dislocation densities in some annealed and cold-worked metals from measurements on the X-ray Debye-Scherrer spectrum, Philos. Mag., 1(1), 1956,34-45. | | 11- S. Ilican, Y. Caglar and M. Caglar, 2008, Preparation and characterization of ZnO thin films deposited by sol-gel spin coating method, J. Optoelectron. Adv. Mater., 10(10), 2578-2583. | 12 .F. Sava, A. Lorinczi, M. Popescu, G. Socol, E. Axente, I. N. Mihailescu, M. Nistor Journal of Optoelectronics and Advanced Materials Vol. 8, No. 4, August 2006, p. 1367 - 1371 |